http://dx.doi.org/10.5012/bkcs.2014.35.12.3437

A Carbazole Based Bimodal "Turn-On" Fluorescent Probe for Biothiols (Cysteine/Homocysteine) and Fluoride: Sensing, Imaging and its Applications

Matinder Kaur, Byungkwon Yoon, Rajesh Kumar, Min Ju Cho, Hak Joong Kim, Jong Seung Kim, and Dong Hoon Choi*

Department of Chemistry, Research Institute for Natural Sciences, Korea University, Seoul 136-701, Korea
**E-mail: dhchoi8803@korea.ac.kr*
Received June 17, 2014, Accepted August 6, 2014

A well-known carbazole-based precursor (probe **1**) was used for the detection of cysteine/homocysteine and fluoride. Probe **1** shows a "turn-on" response to cysteine/homocysteine and fluoride *via* enhancement in emission intensity at 442 nm and 462 nm respectively, in solutions and living cells. Furthermore, probe **1** behaves as a fluorescent molecular switch between cysteine/homocysteine and fluoride as the chemical inputs, which have been used for the development of a combinatorial logic circuit and a molecular keypad lock.

Key Words : Carbazole probe, Cysteine/homocysteine sensing, Fluoride recognition, Molecular keypad lock, Bioimaging

Introduction

Thiols (cysteine, homocysteine, and glutathione) are commonly used as highly active, reduced forms of sulfur found in biomolecules. They play an important role in maintaining redox homeostasis by regulating the redox status between reduced free thiols and oxidized disulfides.[1-3] Thiol deficiency is associated with a number of health problems including slow growth in children, liver damage, and AIDS. In contrast, high thiol levels are responsible for the growth of several other syndromes.[4-7] Therefore, the scientific community has made enormous efforts toward expanding the scope of new fluorescent sensors to quantitatively and selectively detect thiols. Usage of fluorescent probes have advantages over other complicated and tedious methods, as they are capable of detecting these species with high sensitivity in solution as well as in living cells simply by converting the cognitive response into a amenable fluorescence signals.[8-10] In recent years, a number of fluorescent probes for thiols have been developed, but they have certain limitations such as complicated and tedious synthesis with low yields that make their practical application difficult.[11-15]

Recently, significant progress has been made in the fluorogenic detection of anions particularly fluoride ions (F^-).[16-21] Fluoride ions play a dynamic role in chemical, environmental, medical, and biological processes.[22-24] The United States Environmental Protection Agency (EPA) recommends two standard values for F^- concentration in drinking water: 4 mg L^{-1} protect from osteofluorosis and 2 mg L^{-1} to protect against dental fluorosis. Hence, accurate detection of F^- in drinking water is necessary, as concentrations exceeding a maximum limit can be hazardous. Therefore, we have to develop effective method for selective removal of F^- which is an important issue of both medicinal and ecological senses.

Aldehydes are known to react with the N-terminal group of cysteine (Cys) and homocysteine (Hcy) to form thiazolidine and thiazinane, residues respectively.[25,26] With this context in mind, a well-known carbazole-based precursor with dialdehyde functionality was synthesized according to the reported procedure[27] for the detection of Cys/Hcy and F^- under different mechanisms. Therefore, our molecular design was based on the utilization of two reactive sites in probe **1**: –CHO groups, which display high selectivity toward Cys/Hcy, and the –NH group of a carbazole for F^- selectivity (Figure 1). In solutions and living cells, probe **1** exhibited a "turn-on" response to Cys/Hcy and F^- through an enhancement of emission intensity at 442 nm and 462 nm, respectively. It is worth noting that although the formation of thiazolidines or thiazinanes has been often employed in Cys/Hcy probe development,[28-32] this type of probe system has not been demonstrated in molecular logic gates or for the development of combinatorial logic circuits and molecular keypad locks.

Experimental

Reagents and Materials. All solvents used were of analytical grade. Solvents were dried according to standard procedures. ^1H and ^{13}C nuclear magnetic resonance (NMR) spectra were recorded on a Varian Mercury NMR 300 MHz and 400 MHz spectrometer using deuterated dimethylsulfoxide (DMSO-d_6) purchased from Cambridge Isotope Laboratories, Inc. Mass spectra were recorded on a Shimadzu an LCMS-2020 (Liquid Chromatograph Mass Spectrophotometer). UV-vis absorption spectra were obtained using a UV-vis absorption spectrometer (HP 8453, photodiode array type) in the wavelength range of 190-1100 nm. The fluorescence spectra were recorded with a Hitachi F-7000 fluorescence spectrophotometer with a slit width (of 5 nm) used for excitation and emission. Fluorescence images of the cells were recorded on confocal microscope from Leica (Leica TCS SP2 model).

Synthesis of Probe 1. The general synthetic procedure is given in Scheme 1. Probe **1** was synthesized according to the

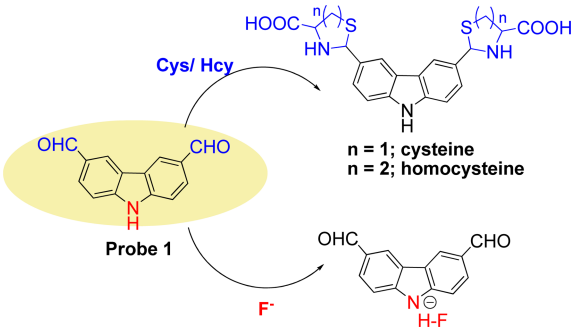

Figure 1. Structure of fluorescent probe **1** and its interactions with thiols and fluoride ions.

reported procedure and characterized by ^{1}H and ^{13}C NMR spectroscopy (see supporting information, Figures S1 and S2).[27] 3,6-Dibromocarbazole (1 g, 3.10 mmol) was dissolved in anhydrous THF (30 mL) to obtain a pale yellow solution, which was stirred at −78 °C (dry ice/acetone bath). A 12 mL solution of *n*-BuLi (1.6 M in hexane) was then added over a period of 10 min, causing the reaction contents to significantly darken in color. The reaction mixture was stirred at room temperature for 1 h. Then, at −78 °C, anhydrous dimethylformamide (2.5 mL) was added over 10 min, immediately causing the precipitation of a pale yellow solid. The cooling bath was removed, and the reaction mixture was stirred for 90 min. After this period, 1 M HCl (20 mL) was added, and the reaction mixture was filtered by suction. The filtrate was extracted with EtOAc (5 × 50 mL), and the combined extract was washed with brine (50 mL), dried over Na_2SO_4 and concentrated to an off-white solid in a yield of 0.99 g (72%). ^{1}H NMR (300 MHz, DMSO-d_6) δ 7.72 (2H, d, J = 6 Hz, ArH), 8.04 (2H, d, J = 6 Hz, ArH), 8.89 (2H, s, ArH), 10.10 (2H, s, CHO), 12.36 (broad, NH); ^{13}C NMR (100 MHz, DMSO-d_6) δ 192.3, 144.5, 129.7, 127.8, 125.2, 125.3, 121.7; ESI-MS (M^+): 223 (M^+).

Experimental Details for Cys/Hcy and Fluoride Detection. A stock solutions (10^{-3} M) of probe **1** were prepared in a DMSO-HEPES buffer (v/v, 3:7, pH 7.4), and the stock solution was further diluted to 3.0 μM concentration for UV–vis absorption spectral studies and to 1.0 μM for fluorescence spectral studies. The (10^{-3} M) stock solutions of the amino acids and tetrabutylammonium fluoride (TBAF) were prepared in a DMSO-HEPES buffer (v/v, 3:7, pH 7.4).

Cell Culture, Treatment of Probe 1 with *N*-Ethyl Maleimide (NEM). A human HeLa cell line was grown in Dulbecco's Modified Eagle medium supplemented with 10% fetal calf serum, 1% penicillin, and 10,000 unit/mL of streptomycin at 37 °C under humidified air containing 5% CO_2. Cells (1.0×10^5) were located and stabilized in a single well of a 24-well plate. When 80% confluence was reached, the cells were washed twice with 1.0 mL of phosphate buffered saline (PBS) and finally incubated with 1.0 mL of PBS containing probe **1** (final concentration of 2.0 μM) for the following confocal experiment. For the NEM treated samples, the cells were incubated with media containing NEM at variable concentrations for 1 h at 37 °C before the media were finally replaced with PBS containing probe **1** (the concentration of its stock solution was 1 mM in DMSO). The fluorescence images in the confocal experiments were obtained at 1 min after the cells were treated with probe **1**.

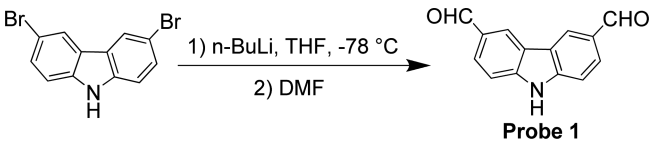

Scheme 1. Synthesis of probe **1**.

Fluorescence Imaging. Fluorescence images of the cells treated with probe **1** were taken using a confocal microscope from leica (Leica TCS SP2 model). The images were obtained within 2 min probe **1** was being added to the cells. The excitation source was a 740 nm argon laser and an emission image was acquired using a long path filter (> 560 nm). All images were taken under the same experimental parameters to minimize possible variations in fluorescence intensity.

Determination of Binding Constants and Detection Limits. The binding constants for probe **1** complexes with Cys and F^- were calculated using the Benesi–Hildebrand equation.[33]

$$1/(A_f - A_{obs}) = 1/(A_f - A_{fc}) + 1/K(A_f - A_{fc})\,[\text{Ligand}]$$

In this equation, A_f is the absorbance of the free host, A_{obs} is the observed absorbance, A_{fc} is the absorbance at saturation, and K is the binding constant.

The detection limit (DL) was determined from a calibration curve of the fluorescence intensity versus Cys and F^- concentrations. Using this plot, the DL was calculated by multiplying the concentration with a sharp change in the fluorescence intensity by the concentration of probe **1**.

The following equation was used for calculating the DL:

$$\text{DL} = \text{CL} \times \text{CT}$$

CL = concentration of ligand; CT = concentration of titrant at which the spectral change was observed.

Results and Discussion

UV–Vis Absorption Studies of Probe 1 with Cysteine and Fluoride. In this work, the photophysical properties of probe **1** (3.0 μM) were studied in the absence or presence of Cys/Hcy in DMSO-HEPES buffer (v/v, 3:7, pH 7.4) at ambient temperature. The absorption spectra of probe **1** showed bands at 261 nm, 292 nm, and 329 nm. Upon incremental addition of Cys (0.01–2 equiv.) to the solution of probe **1**, an overall increase in the absorption was observed and the color of the solution changed from colorless to light yellow, providing a "naked-eye" probe for Cys (Figure 2(a), inset). Job's plot was used to determine the stoichiometry of **1**-Cys complex. The total concentration of probe **1** and Cys was constant (2.5×10^{-6} M), with a continuously varied molar fraction of guest [Cys]/([**1**]+[Cys]). The concentration of **1**-Cys complex approached a maximum when the molar fraction of Cys is 0.7, which indicates that probe **1** and Cys

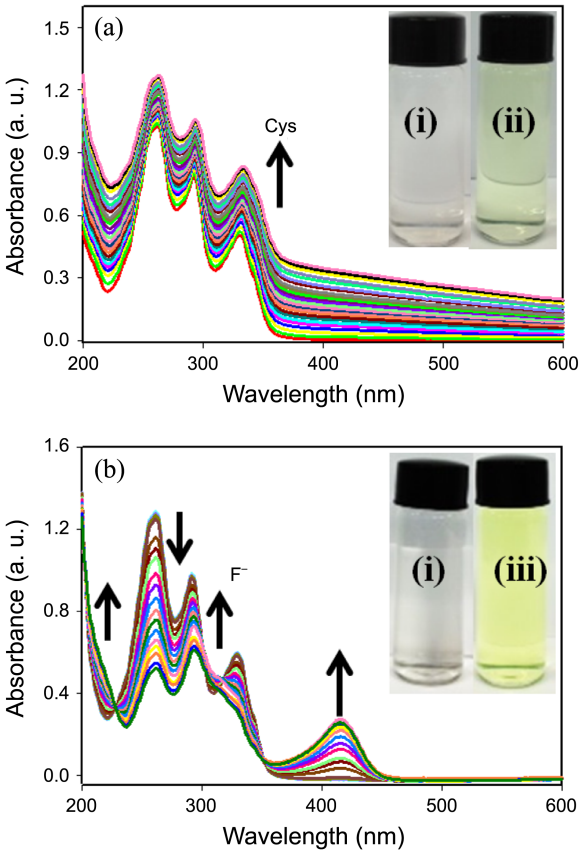

Figure 2. UV-vis absorption spectra of probe **1** (3.0 μM) in a DMSO-HEPES buffer (v/v, 3:7, pH 7.4) upon incremental addition of: (a) Cys (0.01-2 equiv.) and (b) TBAF (0.01-2 equiv.). Inset: Images showing the change in color of (i) probe **1**, (ii) probe **1** with Cys and (iii) probe **1** with TBAF.

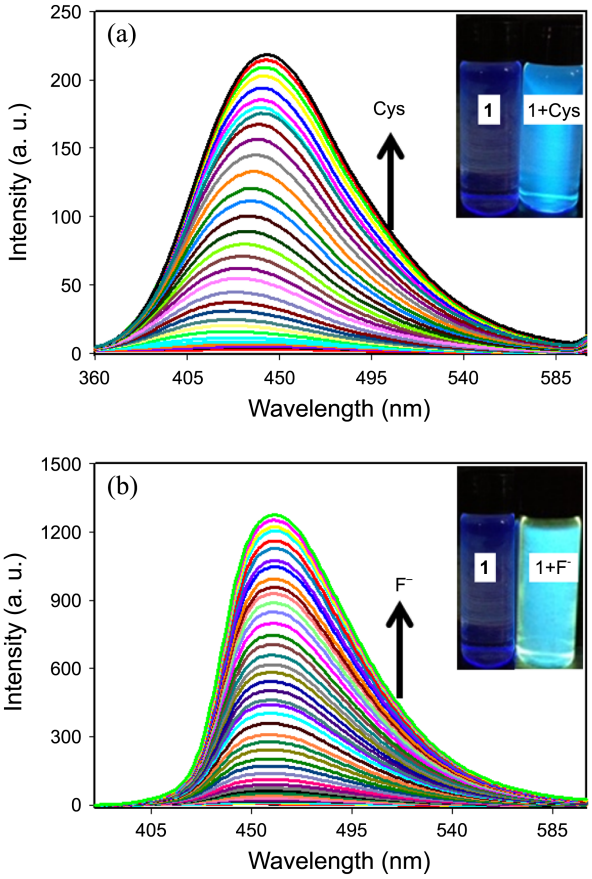

Figure 3. Fluorescence spectra of probe **1** (1.0 μM) in a DMSO-HEPES buffer (v/v, 3:7, λ_{ex} = 300 nm at pH 7.4) upon the addition of: (a) Cys (0.01-3 equiv.) and; (b) TBAF (0.01-4 equiv.). Inset: Emission color change of probe **1** under ultraviolet light before and after the addition of (a) Cys and, (b) TBAF.

form a 1:2 complex as shown in Figure S3 (see supporting information), and the K_a was found to be 1.1×10^7 M^{-1}.

On the other hand, addition of TBAF (0.01–2 equiv.) to the solution of probe **1** resulted in an absorption decrease for the bands at 261 nm, 292 nm, and 329 nm, a small increase at 310 nm, and formation of a new red-shifted charge-transfer (CT) band at 416 nm, that was the result of interaction between probe **1** and F^- which was escorted by a color change from colorless to dark yellow (Figure 2(b), inset). Job's plot was also used to evaluate the 1:1 stoichiometry of the complex formed by probe **1** with F^- as shown in Figure S4 (see supporting information), and the K_a value was 1.3×10^7 M^{-1}.

Fluorescence Studies of Probe 1 with Cysteine and Fluoride. Fluorescence (FL) titrations of probe **1** with Cys were carried out in a DMSO-HEPES buffer (v/v, 3:7, pH 7.4). Upon the incremental addition of Cys (0.01–3 equiv.) to the solution of probe **1** (1.0 μM), the FL intensity at 442 nm increased more than 80-fold (Figure 3(a)). This is due to the formation of a thiazolidine ring that results in the deterioration of the push-pull effect in probe **1**. To confirm the ring formation, probe **1** was reacted with Cys, to give compound **2** which was characterized by ^{1}H NMR spectrum as demonstrated in Scheme S1 (see supporting information). ^{1}H NMR spectrum showed the resonance signal corresponding to the aldehyde proton (H_a) at δ 10.1 ppm which starts disappearing with time and concurrently, two signals at δ 5.43 ppm and at δ 11.91 ppm were assigned to the methine proton (H_b) and carboxylic hydrogen (–COOH), respectively in thiazolidine ring as shown in Figure S5 (see supporting information). The structure of compound **2** was further characterized by conducting mass spectrometry analysis of the reaction mixture, which showed a mass peak at 223, corresponding to the [M^+] of probe **1** as well as a mass peak at 454.25 which corresponds to compound **2** (calculated value 429.086, observed value 454.25 [Compound 2+Na+2H^+] (see supporting information, Figure S6). The UV and FL spectra of compound **2** are given in the Figure S7 (see supporting information). The detection limit of probe **1** as a fluorescent sensor for analysis of Cys was determined to be 0.5×10^{-7} M (see supporting information, Figure S8). The UV-vis absorption and fluorogenic enhancement results of probe **1** with Hcy were shown in Figure S9 (see supporting information).

On the other hand, titrations of probe **1** with TBAF (0.01-4 equiv.) resulted in FL enhancement greater than 540-fold along with a spectral shift from λ_{em} = 442 nm to 462 nm

(Figure 3(b)). The detection limit of probe **1** as a fluorescent sensor for analysis of F^- was determined to be 6.0×10^{-8} M (see supporting information, Figure S10). The FL enhancement was originated from the deprotonation of the –NH group in the carbazole moiety, which increases the electron density on the nitrogen atom and is associated with an enhancement of the push-pull effect through internal charge transfer. The appearance of a yellow color was observed with the FL enhancement. The deprotonation of –NH in probe **1** was also confirmed with ^{1}H NMR studies (Figure S11).

Selectivity and Competitive Experiment of Probe 1. To study the selectivity of probe **1** for other amino acids, we measured the FL intensity changes after the addition of 20 equivalents of each amino acid. No amino acid except Hcy, Cys, and GSH, induced any significant increase in the FL intensity of probe **1** (see supporting information, Figure S12). In order to evaluate the recognition specificity of probe **1** for other thiols such as mercaptoethanol (MER), thioglycerol (TGOL), dithiothreitol (DTT), bovine serum albumin (BSA), under similar conditions, we performed the selectivity experiment of probe **1** in the presence of 20 equivalents of these thiols. Probe **1** does not show any significant response in the fluorescence intensity with these thiols (see supporting information, Figure S12). We further evaluated the selectivity of probe **1** toward F^- in media with other competitive anions (see supporting information, Figure S13). Significant FL enhancement was only observed in the presence of fluoride. Further, to examine the reaction time of probe **1** towards Cys/Hcy and F^-, we carried out time-dependent analysis. The fluorescence responses at 442 nm for Cys/Hcy and at 462 nm for F^- were plotted as a function of time. Reaction of probe **1** (1 μM) with Cys (3 equiv.) resulted in increase in emission intensity and the intensity reaches a maximum within 1 min. In case of Hcy, the reaction was completed in two minutes as shown in Figure S14 (see supporting information). The conversion of probe **1** to compound **2** was very fast due to the formation of a five-membered thiazolidine ring as compared to the formation of six-membered ring of thiazinane with Hcy. However, reaction of probe **1** (1 μM) with F^- (4 equiv.) showed emission maximum in less than a minute (see supporting information, Figure S15).

Molecular Logic Gate and Molecular Keypad Lock. Recently, significant developments have been made in utilizing the supramolecular systems as molecular logic gates and molecular keypad locks.[34-37] These systems transform chemically encoded information (input), into fluorescent signals (output), allowing for the development of molecular level electronic and photonic devices.

In order to explore probe **1** as molecular logic gate and molecular keypad lock, we further investigated the "Off-On" switching process of probe **1** using Cys and F^- as chemical inputs at different wavelengths, since probe **1** shows optical sensing toward Cys and F^- ions at different wavelengths. In the first sequence, Cys (3 equiv.) was added to the solution of probe **1** resulting in the enhancement of fluorescence

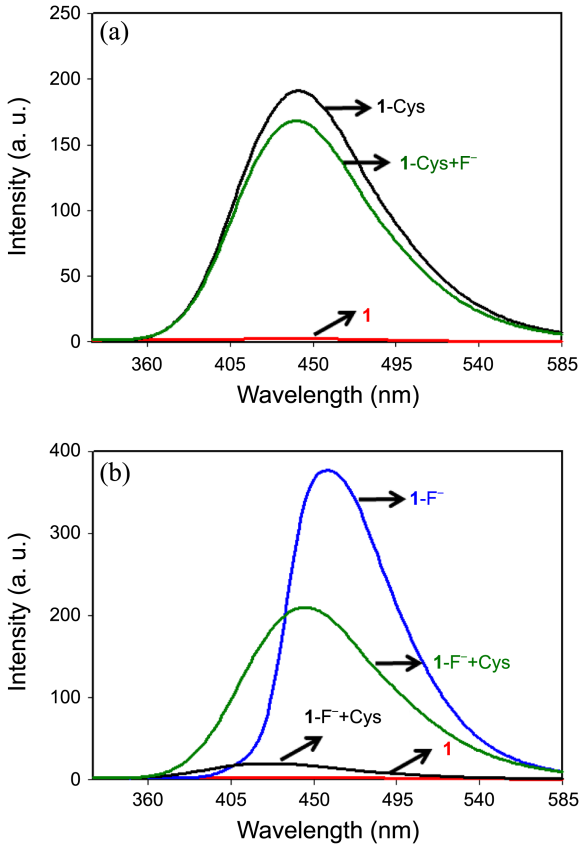

Figure 4. Fluorescence spectra of probe **1** (1.0 μM, red line) and (a) **1**-Cys complex (black line) upon the addition of TBAF (2 μM, green line), and (b) **1**-F^- complex (blue line) upon the addition of Cys (1 μM, black line, and 2 μM, green line) in a DMSO-HEPES buffer (v/v, 3: 7, pH 7.4, λ_{ex} = 300 nm).

intensity at 442 nm due to the formation of **1**-Cys complex (Figure 4(a), black line) and sequential addition of F^- to the solution of **1**-Cys complex, exhibited no significant change in the emission band at 442 nm (Figure 4(a), green line). This is due to formation of thiazolidine ring, which inhibits the push-pull effect of F^-. Therefore, when F^- was added, there was no electron transfer from the carbazole to the thiazolidine ring and no change in the FL of **1**-Cys was observed. On the other hand, in the reverse input sequence, the addition of 4 equiv. of F^- to the solution of probe **1** resulted in the enhancement of fluorescence intensity at 462 nm (Figure 4(b), blue line). Sequential addition of Cys (1 μM) to the solution of **1**-F^- induced the quenching of FL at 462 nm due to a weakening of the push-pull effect of F^- resulting from the formation of thiazolidine ring (Figure 4(b), black line) and further addition of Cys (2 μM) induces enhancement of FL intensity at λ_{em} = 442 nm (Figure 4(b), green line).

Therefore, depending on the two chemical inputs, Cys and F^-, probe **1** can switch between different FL emission states, i.e. "On" (strong FL emission) or "Off" (FL quenching). The "Off-On" switching behavior of probe **1** can be demonstrated using binary logic. The two chemical inputs Cys and F^- were denoted as *In*C and *In*F, respectively, and are

Table 1. Truth Table

Entry	Input-1 Cys (*In*C)	Input-2 F^- (*In*F)	Output-1 442 nm	Output-2 462 nm
1	0	0	0	0
2	1	0	1	0
3	0	1	0	1
4	1[a]	1	1	0

[a]added first

considered to be "1" if the inputs are present and "0" if they are absent. The output signals were measured as the FL emissions at 442 and 462 nm, and considered as "1" when the FL intensity was high, and "0" if it was low. For the first input sequence, the addition of *In*C (Cys) followed by *In*F (F^-) led to no change in the FL emission at 442 nm, and the output was "1" ("On" state, Table 1).

As shown in the constructed combinatorial logic circuit (Figure 5), in the absence of either one of the chemical inputs (*In*C and *In*F), no characteristic bands were observed at 442 nm and 462 nm, *i.e.*, outputs 1 and 2 become "0". With the operation of Cys to the **1**-F^- complex, output 2 became "0", at 462 nm, but the FL emission at 442 nm went to the "ON" state and the output 1 was "1". The output 1 at 442 nm is activated by a combination of the OR and AND gate. However, the output 2 at 462 nm of probe **1** with chemical inputs of *In*F and *In*C is activated through an INHIBIT logic gate. The combination of these intrinsic properties with the selective actions based on the chemical input allows for the design of a complex molecular switch. Further, the change in fluorescence behavior of probe **1** with Cys and F^- has been used to mimic a molecular keypad lock. The chemical inputs Cys and F^- were represented as "G" and "E", respectively. The output signals were represented by letters "T" (strong fluorescence emission at 442 nm, On-state) and "O" (quenched fluorescence emission at 462 nm, Off-state) respectively. The first input sequence "G" followed by input "E" (*i.e.* Cys was first added to the solution of probe **1** followed by the addition of F^- to the solution of **1**-Cys complex) led to strong emission at 442 nm as discussed in Figure 4(a) (On state, represented by letter "T") which produces a green signal at the top of the keypad lock indicating the correct password "GET" (Figure 6). Upon adding the inputs in a reverse sequence "E" followed by input "G"), (*i.e.* F^- was first added to the solution of probe **1** followed by the addition of Cys to the solution of **1**-F^- complex) resulted

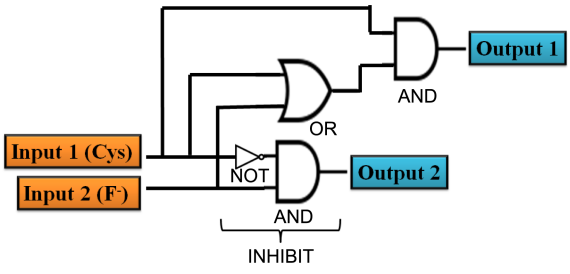

Figure 5. Combinatorial logic circuit diagram.

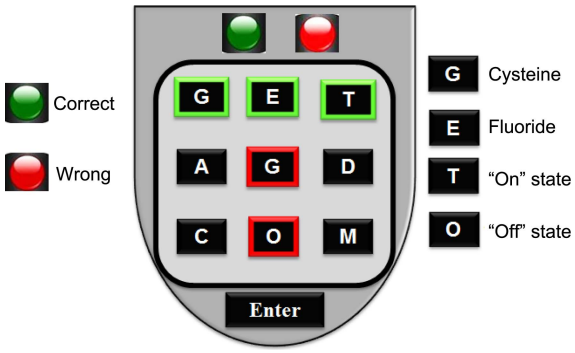

Figure 6. Diagrammatic representation of a molecular keypad lock operated with probe **1**.

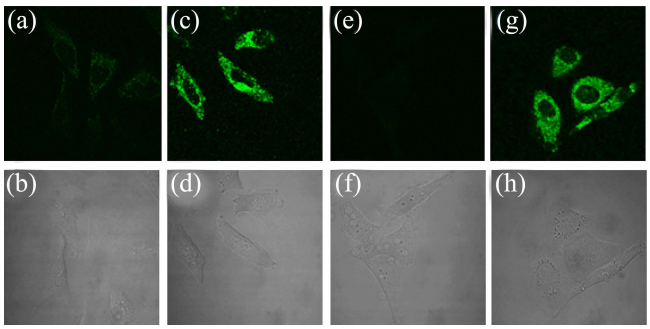

Figure 7. Fluorescence images and bright-field images of HeLa cells (a, b) incubated with 2 μM of probe **1**; (c, d) pretreated with probe **1** (2 μM), then incubated with NaF (100 μM); (e, f) pretreated with 1 mM NEM for 30 min; (g, h) and then incubated with 2 μM of probe **1** and (200 μM) cysteine for 15 min.

in the FL quenching as discussed in Figure 4(b) (Off state, represented by letter "O") which produces a red signal at the top of the keypad lock indicating the wrong password "EGO" unable to open the lock. Thus, an exact sequence would be possible by assigning the correct order of input signals (Cys and F^-), to open the security keypad lock.

Bioimaging. To examine the practicability of probe **1** for detecting Cys/F^- in living cells, confocal microscopy experiments were conducted. The FL and bright field images obtained from HeLa cells were shown in Figure 7. Upon incubation with 2 μM of probe **1** for 20 min at 37 °C, the cells displayed very weak intracellular FL (Figure 7(a)). In the same way, when these treated cells were further treated with NaF (100 μM) for 15 min, an intense green FL signal was observed (Figure 7(c)). This experiment demonstrates that probe **1** is capable of imaging F^- in living cells. In order to confirm whether probe **1** is specific to intracellular Cys/Hcy, a control experiment was conducted by removing the intracellular thiols using 1 mM *N*-methylmaleimide (NEM, a thiol-blocking reagent) prior to incubation of the cells with probe **1** and then the images were recorded which showed marked FL quenching (Figure 7(e)). Further, NEM treated HeLa cells were incubated with Cys (200 μM), immediately FL enhancement was observed which corresponds to the adduct of probe **1** and Cys/Hcy (Figure 7(g)). These results revealed that the probe could indeed react with intracellular

Cys/Hcy to produce FL.

Conclusion

In summary, we here report the application of a well-known precursor as a selective bimodal "turn-on" probe for the detection of Cys/Hcy and fluoride in living cells. The simple synthesis could be scaled up to produce very large amounts of probe **1**. Furthermore, probe **1** behaves as a molecular switch with Cys and F^- chemical inputs forming a combinatorial logic circuit and a molecular keypad. The system could be employed for creating security devices.

Acknowledgments. The authors acknowledge the financial support from the National Research Foundation of Korea (NRF2012R1A2A1A01008797) and by Key Research Institute Program through the National Research Foundation of Korea (NRF) funded by the Ministry of Education, Science and Technology (NRF20100020209).

References

1. Berndt, C.; Lillig, C. H.; Holmgren, A. *Am. J. Physiol. Heart Circ. Physiol*. **2007**, *292*, H1227.
2. Brosnan, J. T.; Brosnan, M. E. *J. Nutr*. **2006**, *136*, 1636S.
3. Moriarty-Craige, S. E.; Jones, D. P. *Ann. Rev. Nutr*. **2004**, *24*, 481.
4. Prakash, M.; Shetty, M. S.; Tilak, P.; Anwar, N. *OJHAS* **2009**, *8*, 2.
5. Masella, R.; Mazza, G. *Glutathione and Sulfur Amino Acids in Human Health and Disease*; 2008, ISBN: 9780470170854.
6. Zhang, S.; Ong, C. N.; Shen, H. M. *Cancer Lett.* **2004**, *208*, 143.
7. Kovar, J.; Stybrova, H.; Truksa, J.; Spevakova, K.; Valenta, T. *Folia Biol*. **2002**, *48*, 58.
8. Ueno, T.; Nagano, T. *Nat. Methods* **2011**, *8*, 642.
9. Kobayashi, H.; Ogawa, M.; Alford, R.; Choyke, P. L.; Urano, Y. *Chem. Rev.* **2010**, *110*, 2620.
10. Rao, J.; Dragulescu-Andrasi, A.; Yao, H. *Curr. Opin. Chem. Biol*. **2007**, *18*, 17.
11. Shi, J.; Wang, Y.; Tang, X.; Liu, W.; Jiang, H.; Dou, W.; Liu, W. *Dyes Pigm.* **2014**, *100*, 255.
12. Yuan, Y.; Kwok, R. T. K.; Feng, G.; Liang, J.; Geng, J.; Tang, B. Z.; Liu, B. *Chem. Commun*. **2014**, 295.
13. Liu, Y.; Zhang, S.; Lv, X.; Sun, Y.-Q.; Liu, J.; Guo, W. *Analyst* **2014**, *139*, 4081.
14. Song, Q.-H.; Wu, Q. Q.; Liu, C.-H.; Du, X.-J.; Guo, Q.-X. *J. Mater. Chem. B* **2013**, *1*, 438.
15. Isik, M.; Ozdemir, T.; Turan, I. S.; Kolemen, S.; Akkaya, E. U. *Org. Lett.* **2013**, *15*, 216.
16. Ashokkumar, P.; Weißhoff, H.; Kraus, W.; Rurack, K. *Angew. Chem. Int. Ed.* **2014**, *53*, 2225.
17. Kaur, M.; Cho, M. J.; Choi, D. H. *Dyes Pigm.* **2014**, *103*, 154.
18. Roy, A.; Datar, A.; Kand, D.; Saha, T.; Talukdar, P. *Org. Biomol. Chem.* **2014**, *12*, 2143.
19. Yuan, M. S.; Wang, Q.; Wang, W.; Wang, D. E.; Wang, J.; Wang, J. *Analyst* **2014**, *139*, 1541.
20. Saravanan, C.; Easwaramoorthi, S.; Hsiow, C. Y.; Wang, K.; Hayashi, M.; Wang, L. *Org. Lett*. **2014**, *16*, 354.
21. Cametti, M.; Rissanen, K. *Chem. Soc. Rev.* **2013**, *42*, 2016.
22. Farley, J. R.; Wergeda, J. E.; Baylink, D. J. *Science* **1983**, *222*, 330.
23. Horowitz, H. S. *J. Public Health Dent.* **2003**, *63*, 3.
24. Lennon, M. A. *Bull. World Health Organ.* **2006**, *84*, 759.
25. Schubert, M. P. *J. Biol. Chem*. **1936**, *114*, 341.
26. Schubert, M. P. *J. Biol. Chem.* **1937**, *121*, 539.
27. Folmer-Andersen, J. F.; Buhler, E.; Candau, S. J.; Joulie, S.; Schmutz, M.; Lehn, J. M. *Polym. Int.* **2010**, *59*, 1477.
28. Goswami, S.; Manna, A.; Paul, S.; Das, A. K.; Nandi, P. K.; Maity, A. K.; Saha, P. *Tetrahedron Lett.* **2014**, *55*, 490.
29. Son, S.-H.; Kim, Y.; Heoc, M. B.; Lim, Y. T.; Lee, T. S. *Tetrahedron* **2014**, *70*, 2034.
30. Kong, F.; Liu, R.; Chu, R.; Wang, X.; Xu, K.; Tang, B. *Chem. Commun*. **2013**, 9176.
31. Das, P.; Mandal, A. K.; Chandar, N. B.; Baidya, M.; Bhatt, H. B.; Ganguly, B.; Ghosh, S. K.; Das, A. *Chem. Eur. J.* **2012**, *18*, 15382.
32. Yang, Z.; Zhao, N.; Sun, Y.; Miao, F.; Liu, Y.; Liu, X.; Zhang, Y.; Ai, W.; Song, G.; Shen, X.; Yu, X.; Sun, J.; Wong, W. Y. *Chem. Commun.* **2012**, 3442.
33. Hildebrand, J. H.; Benesi, H. A. *J. Am. Chem. Soc.* **1949** *71*, 2703.
34. Bhalla, V.; Roopa, Kumar, M. *Org. Lett.* **2012**, *14*, 2802.
35. Szacilowski, K. *Chem. Rev.* **2008**, *108*, 3481.
36. *Molecular Devices and Machines. A Journey into the Nano World*; Balzini, V., Venturi, M., Credi, A., Eds.; Wiley-VCH: Wienheim, 2003.
37. Mitchell, R. J. *Microprocessor Systems: An Introduction*; Macmillan: London, 1995.